SLAC–PUB–9289
July 2002

Measurement of the Double-inclusive $b\bar{b}$ Quark Fragmentation Function in Z^0 decays and First Measurement of Angle Dependant $B - \overline{B}$ Energy Correlations*

The SLD Collaboration**
Stanford Linear Accelerator Center
Stanford University, Stanford, CA 94309

ABSTRACT

We present preliminary results of a measurement of the double-inclusive $b\bar{b}$ quark fragmentation function in Z^0 decays using a novel kinematic B hadron energy reconstruction technique. The measurement is performed using 350,000 hadronic Z^0 events recorded in the SLD experiment at SLAC between 1996 and 1998. The small and stable SLC beam spot and the CCD-based vertex detector are used to reconstruct topological B-decay vertices with high efficiency and purity, and to provide precise measurements of the kinematic quantities used in this technique. We measure the B energy with good efficiency and resolution over the full kinematic range. We present a preliminary measurement of the angle dependent correlations between the B and $\bar{B}$ hadron energies in $Z^0 \rightarrow b\bar{b}$ events, and compare with the leading order QCD predictions.

Contributed to the International Conference on High Energy Physics, 24-31 July, 2002, Amsterdam, The Netherlands.

* Work supported in part by Department of Energy contract DE-AC03-76SF00515.

1. Introduction

The production of heavy hadrons (H) in e^+e^- annihilation provides a laboratory for the study of heavy-quark (Q) jet fragmentation. This is commonly characterized in terms of the observable $x_H \equiv 2E_H/\sqrt{s}$, where E_H is the energy of a B or D hadron containing a b or c quark, respectively, and $\sqrt{s}$ is the c.m. energy. In recent publications we presented [1] the results of a new method for reconstructing B hadron decays, and the B energy, inclusively, using only charged tracks, in the SLD experiment at SLAC. We use the upgraded CCD vertex detector, installed in 1996, to reconstruct B-decay vertices with high efficiency and purity. Combined with the micron-size SLC interaction point (IP), precise vertexing allows us to reconstruct accurately the B flight direction and hence the transverse momentum of tracks associated with the vertex with respect to this direction. Using the transverse momentum and the total invariant mass of the associated tracks, an upper limit on the mass of the missing particles is found for each reconstructed B-decay vertex, and is used to solve for the longitudinal momentum of the missing particles, and hence for the energy of the B hadron. In order to improve the B sample purity and the reconstructed B hadron energy resolution, B vertices with low missing mass are selected. Our previous studies obtained the world's most precise measurement of the b-quark fragmentation function, and excluded many models not consistent with data. Additionally, the measurement reduces the systematic errors in many areas of B physics at the Z^0 and will improve studies at the Tevatron and B factories.

Existing calculations and models of b fragmentation are almost always dominated by perturbative gluon radiation from the $b\bar{b}$ system well before the formation of B hadrons. Hard gluon radiation affects both the B and $\bar{B}$ energies, and the effect may be studied in detail using the double inclusive B energy distribution. Obtaining the correlation allows us to test the ansatz of factorization in QCD [2], and will be important in systematic errors on precision Electroweak measurements at the Z^0 as well as for the Tevatron and B factories. Until recently, however, there has not been a technique available to reliably measure the distribution with sufficient statistics.

Here we report the study of events in which we reconstructed the energies of both leading B hadrons produced via $e^+e^- \to b\bar{b} \to B\overline{B} + X$. As proposed in [2], we have compared the moments of the single inclusive B hadron distribution dN/dx_B:

$$D_i \quad \equiv \quad \int x_B^i dN/dx_B \; dx_B \tag{1}$$

with the angle dependent moments of the double inclusive scaled-energy distribution $d^2N/dx_{B1}dx_{B2}$:

$$D_{ij}(\phi) \quad \equiv \quad \int\int x_{B1}^i x_{B2}^j d^2N(\phi)/(dx_{B1}dx_{B2}) \; dx_{B1}dx_{B2}, \tag{2}$$

where x_{B1} and x_{B2} are the scaled energies of the two arbitrarily labeled B hadrons, ϕ is the angle between the two hadrons, and i,j=1,2,3 and tested the ansatz of factorization as applied to perturbative QCD calculations of $e^+e^- \to b\bar{b}\ (g)$ events.

2. Apparatus and Hadronic Event Selection

This analysis is based on roughly 350,000 hadronic events produced in e^+e^- annihilations at a mean center-of-mass energy of $\sqrt{s} = 91.28$ GeV at the SLAC Linear Collider (SLC), and recorded in the SLC Large Detector (SLD) in 1997 and 1998. A general description of the SLD can be found elsewhere [3]. The trigger and initial selection criteria for hadronic Z^0 decays are described in Ref. [4]. This analysis used charged tracks measured in the Central Drift Chamber (CDC) [5] and in the upgraded Vertex Detector (VXD3) [6]. Momentum measurement is provided by a uniform axial magnetic field of 0.6T. The CDC and VXD3 give a momentum resolution of $\sigma_{p_\perp}/p_\perp = 0.01 \oplus 0.0026 p_\perp$, where $p_\perp$ is the track momentum transverse to the beam axis in GeV/c. In the plane normal to the beamline the centroid of the micron-sized SLC IP is reconstructed from tracks in sets of approximately thirty sequential hadronic Z^0 decays to a precision of $\sigma^{r\phi} \simeq 4$ μm. The IP position along the beam axis is determined event by event using charged tracks with a resolution of $\sigma^z \simeq 20$ μm. Including the uncertainty on the IP position, the resolution on the charged-track impact parameter (d) projected in the plane perpendicular to the beamline is $\sigma_d^{r\phi} = 8 \oplus 33/(p \sin^{3/2}\theta)$ μm, and the resolution in the plane containing the beam axis is $\sigma_d^z = 10 \oplus 33/(p \sin^{3/2}\theta)$ μm, where θ is the track polar angle with respect to the beamline. The event thrust axis [7] is calculated using energy clusters measured in the Liquid Argon Calorimeter [8].

A set of cuts is applied to the data to select well-measured tracks and events well contained within the detector acceptance. Charged tracks are required to have a distance of closest approach transverse to the beam axis within 5 cm, and within 10 cm along the axis from the measured IP, as well as $|\cos\theta| < 0.80$, and $p_\perp > 0.15$ GeV/c. Events are required to have a minimum of seven such tracks, a thrust axis polar angle w.r.t. the beamline, θ_T, within $|\cos\theta_T| < 0.71$, and a charged visible energy E_{vis} of at least 20 GeV, which is calculated from the selected tracks assigned the charged pion mass. The efficiency for selecting a well-contained $Z^0 \to q\bar{q}(g)$ event is estimated to be above 96% independent of quark flavor. The selected sample comprised 218,953 events, with an estimated $0.10 \pm 0.05\%$ background contribution dominated by $Z^0 \to \tau^+\tau^-$ events.

For the purpose of estimating the efficiency and purity of the selection procedures we made use of a detailed Monte Carlo (MC) simulation of the detector. The JETSET 7.4 [9] event generator is used, with parameter values tuned to hadronic e^+e^- annihilation data [10], combined with a simulation of B hadron decays tuned [11] to $\Upsilon(4S)$ data and a simulation of the SLD based on GEANT 3.21 [12]. Inclusive distributions of single-particle and event-topology observables in hadronic events are found to be well described by the simulation [4]. Uncertainties in the simulation are taken into account in the systematic errors (Section 5).

3. B Hadron Selection and Energy Measurement

The event sample for this analysis is selected using a topological vertexing technique based on the detection and measurement of charged tracks, which is described in detail in Ref. [13]. We considered events in which we found secondary vertices corresponding to both the leading B and $\bar{B}$ hadrons. The Durham algorithm was first applied to the selected hadronic events, with a y_c parameter value of 0.015, in order to define a jet structure in each event. We use the Durham algorithm because it minimizes the number of B and D decay tracks assigned to the wrong jet, with respect to other jet finders. This is an important feature for our analysis because we only use event variables derived from reconstructed tracks. The topological vertexing algorithm is applied to the set of 'quality' tracks in each jet having (i) at least 23 hits in the CDC and 2 hits in VXD3; (ii) a combined CDC and VXD3 track fit quality of χ^2/N_{dof} <8; (iii) a momentum in the range 0.25< p <55 GeV/c, (iv) an impact parameter of less than 0.3 cm in the $r\phi$ plane, and less than 1.5 cm along the z axis; (v) a transverse impact parameter error no larger than 250 μm. Vertices consistent with photon conversions or K^0 and Λ^0 decays are discarded. Events were retained in which a secondary vertex was found in exactly two of the reconstructed jets.

The large masses of the B hadrons relative to light-flavor hadrons make it possible to distinguish B hadron decay vertices from those vertices found in events of light flavors using the vertex invariant mass, M. However, due to the missing particles, which are mainly neutrals, M cannot be fully determined. M can be written as

$$M = \sqrt{M_{ch}^2 + P_t^2 + P_{chl}^2} + \sqrt{M_0^2 + P_t^2 + P_{0l}^2} \qquad (3)$$

where M_{ch} and M_0 are the total invariant masses of the set of vertex-associated tracks and the set of missing particles, respectively. P_t is the total charged track momentum transverse to the B flight direction, which is identical to the transverse momentum of the set of missing particles by momentum conservation. P_{chl} and P_{0l} are the respective momenta along the B flight direction. In the B *rest* frame, $P_{chl} = P_{0l}$. Using the set of vertex-associated charged tracks, we calculate the total momentum vector $\vec{P}_{ch}$ and its component transverse to the flight direction P_t, and the total energy E_{ch} and invariant mass M_{ch}, assuming the charged pion mass for each track. The lower bound for the mass of the decaying hadron, the 'P_t-corrected vertex mass',

$$M_{Pt} = \sqrt{M_{ch}^2 + P_t^2} + |P_t| \qquad (4)$$

is used as the variable for selecting B hadrons. The majority of non-B vertices have M_{Pt} less than 2.0 GeV/c^2. However, occasionally the measured P_t may fluctuate to a much larger value than the true P_t, causing some charm vertices to have a M_{Pt} larger than 2.0 GeV/c^2. To reduce this contamination, we calculate the 'minimum P_t' by allowing the locations of the IP and the vertex to float to any pair of locations within the respective one sigma error-ellipsoids, We substitute the minimum P_t in Equation (4) and use the modified M_{Pt} as our variable for selecting B hadrons.

The energy of each B hadron, E_B, can be expressed as the sum of the reconstructed-vertex energy, E_{ch}, and the energy of those particles not associated with the vertex, E_0. We can write E_0 as

$$E_0^2 = M_0^2 + P_t^2 + P_{0l}^2 \tag{5}$$

The two unknowns, M_0 and P_{0l}, must be found in order to obtain E_0. One kinematic constraint can be obtained by imposing the B hadron mass on the vertex, $M_B^2 = E_B^2 - P_B^2$, where $P_B = P_{chl} + P_{0l}$ is the total momentum of the B hadron, and P_{chl} is the momentum component of the vertex-associated tracks along the vertex axis. From Equation (3) we derive the following inequality,

$$\sqrt{M_{ch}^2 + P_t^2} + \sqrt{M_0^2 + P_t^2} \leq M_B, \tag{6}$$

where equality holds in the limit where both P_{0l} and P_{chl} vanish in the B hadron *rest* frame. Equation (6) effectively sets an upper bound on M_0, and a lower bound is given by zero:

$$0 \leq M_0^2 \leq M_{0max}^2, \tag{7}$$

where

$$M_{0max}^2 = M_B^2 - 2M_B\sqrt{M_{ch}^2 + P_t^2} + M_{ch}^2. \tag{8}$$

Since M_0 is bounded from both above and below, we expect to obtain a good estimate of M_0, and therefore of the B hadron energy, when M_{0max}^2 is small.

Because M_0 peaks near M_{0max}, [14] we set $M_0^2 = M_{0max}^2$ if $M_{0max}^2 \geq 0$, and $M_0^2 = 0$ if $M_{0max}^2 < 0$. We then calculate P_{0l}:

$$P_{0l} = \frac{M_B^2 - (M_{ch}^2 + P_t^2) - (M_0^2 + P_t^2)}{2(M_{ch}^2 + P_t^2)} P_{chl}, \tag{9}$$

and hence E_0 (Equation (5)). We then divide the reconstructed B hadron energy, $E_B^{rec} = E_0 + E_{ch}$, by the beam energy, $E_{beam} = \sqrt{s}/2$, to obtain the reconstructed scaled B hadron energy, $x_B^{rec} = E_B^{rec}/E_{beam}$.

A number of cuts was then applied to the data to maximize our efficiency for finding both vertices, and reducing backgrounds. Events were retained in which secondary vertices were found in exactly two jets, at least 1 mm from the interaction point, and where both reconstructed B energies satisfied $0 < E_B^{rec} < 60$ GeV.

Both vertices were then required to satisfy $-1 < M_{0max}^2 < 12$ (GeV/c^2)^2. Lower values of M_{0max}^2 correspond to improved energy resolution, and higher values correspond to improved selection efficiency. We performed a Monte Carlo study to find the optimum range such that the statistical errors on the moments of the distribution were minimized but still insensitive to the uncertainty in the energy measurement.

The angle, ϕ, between the vertex axes of the two B hadrons satisfied cos$\phi < 0.99$, eliminating events in which we found two vertices from the same $B/\bar{B}$ hadron. At least one vertex was required to contain at least two tracks with a normalized impact-parameter significance of 2σ or greater w.r.t. the IP, and at least one vertex to satisfy

$M_{Pt} > 2$ GeV/c^2. These cuts reduced background from $Z^0 \rightarrow c\bar{c}$ and other light quark events which tend to be found with low mass, and close to the interaction point.

A sample of 17707 events was selected, estimated to be 99.9% pure in $Z^0 \rightarrow b\bar{b}$ events, the background being composed of $c\bar{c}$ events, and the efficiency for selecting a true $b\bar{b}$ event was estimated to be 32%.

4. Measurement of the Angle Dependant B-$\overline{B}$ Energy Correlations

We quantified the correlations between the two B hadrons in terms of the angle dependant scaled-energy moments proposed in [2]. We formed the single inclusive B-energy distribution and evaluated the moments (Eq. 1) from the raw measured distribution. The procedure was the same as described in [1], except that instead of Eq. 8 therein we imposed the requirement $M^2_{0max} < 15\mathrm{GeV}^2/\mathrm{c}^4$ in order to increase the statistical precision of the calculation. The moments

$$D_i^{rec} \equiv \int (x_B^{rec})^i dN/dx_B^{rec}\, dx_B^{rec},$$

were evaluated, from which we calculated the factors M_i^{rec}, where

$$D_i^{rec} = M_i^{rec} P_i$$

and the P_i were evaluated at leading order in pQCD and are tabulated in [2].

We next evaluated the double moments using the selected sample (Eq. 2):

$$D_{ij}^{rec}(\phi) \equiv \int\int (x_{B1}^{rec})^i (x_{B2}^{rec})^j d^2N(\phi)/(dx_{B1}^{rec} dx_{B2}^{rec})\, dx_{B1}^{rec} dx_{B2}^{rec},$$

where x_{B1}^{rec} and x_{B2}^{rec} are the reconstructed scaled energies of the two B hadrons, ϕ is the angle between the two vertex axes, and i,j = 1,2,3.

We then formed the quantities:

$$P_{ij}^{rec}(\phi) = D_{ij}^{rec}(\phi)/(M_i^{rec}\, M_j^{rec})$$

and corrected them for detector acceptance and resolution using a standard bin-by-bin method. The corrected, normalized quantities $P_{ij}(\phi)/P_{11}(\phi)$ are shown in Fig. 1. The size of correction applied varies depending on the moment and angle bin. The P_{11} moment correction is unity for $\cos\phi = -1$ but increases until $\cos\phi = +1$ when a factor 1.5 must be applied to take account of detector effects. A similar pattern is seen for the P_{22} and P_{31} moments. The P_{21} (P_{32},P_{33}) moment has a correction factor ranging from 1 to 1.25 (1.25 to 2.5) over the full angular range. There is only a small change in the correction factor if a different fragmentation model is assumed, and the associated uncertainty on the final result is estimated as a systematic error.

5. Systematic Errors

We have considered sources of systematic uncertainty that potentially affect our measurement. These may be divided into uncertainties in modeling the detector and uncertainties on experimental measurements serving as input parameters to the underlying physics modeling. For these studies our standard simulation, employing the Peterson fragmentation function, is used.

Due to the strong dependence of our energy reconstruction technique on charged tracks, the dominant systematic error is due to the discrepancy in the charged track transverse momentum resolution between the Monte Carlo and the data. We evaluate this conservatively by taking the full difference between the nominal results and results using a resolution-corrected Monte Carlo event sample. The difference between the measured and simulated charged track multiplicity as a function of $\cos\theta$ and momentum is attributed to an unsimulated tracking inefficiency correction. We use a random track-tossing procedure to evaluate the difference in our results.

A large number of measured quantities relating to the production and decay of charm and bottom hadrons are used as input to our simulation. In $b\bar{b}$ events we have considered the uncertainties on: the branching fraction for $Z^0 \to b\bar{b}$; the rates of production of $B^{\pm}$, B^0 and B^0_s mesons, and B baryons; the lifetimes of B mesons and baryons; and the average B hadron decay charged multiplicity. In $c\bar{c}$ events we have considered the uncertainties on: the branching fraction for $Z^0 \to c\bar{c}$; the charmed hadron lifetimes, the charged multiplicity of charmed hadron decays, the production of K^0 from charmed hadron decays, and the fraction of charmed hadron decays containing no π^0s. We have also considered the rate of production of $s\bar{s}$ in the jet fragmentation process, and the production of secondary $b\bar{b}$ and $c\bar{c}$ from gluon splitting. The world-average values [1] of these quantities used in our simulation, as well as the respective uncertainties, are listed in Table 1.

Other relevant systematic effects such as variation of the event selection cuts and the assumed B hadron mass are also found to be very small. As a cross-check, we vary the M_{0max} cut used in selecting the final B sample within a large range and repeat the analysis procedure. For each systematic error and cross-check, the shape of the angular dependence of the momentum correlations is not significantly changed, only the overall normalization is effected. In each angle bin (Fig. 1), all sources of systematic uncertainty are added in quadrature to obtain the total systematic error.

6. Results

The data were compared with a LO pQCD calculation [2] of the corresponding normalized double moments, which is also shown in Fig. 1. The calculation reproduces the data. This result verifies the ansatz of factorization between the perturbative and non-perturbative phases that was the basis of the pQCD calculation of b fragmentation.

Source	Variation
Tracking efficiency correction	-1.5±0.75%
Impact parameter smearing in z	9.0±4.5μm
Track polar angle smearing	1.0±0.5 mrad
Track $1/p_\perp$ smearing	0.8±0.4 MeV^{-1}
B^+ production fraction	0.39±0.11
B^0 production fraction	0.39±0.11
B_s production fraction	0.098±0.0012
Λ_b production fraction	0.103±0.018
$B\to$ charm multiplicity and species	[14]
$B\to K^0$ multiplicity	0.658±0.066
$B\to \Lambda^0$ multiplicity	0.124±0.008
B decay $< n_{ch} >$	4.955±0.062
$D \to K^0$ multiplicity	[14]
$D \to$ no π^0 fraction	[14]
D decay $< n_{ch} >$	[14]
$g \to b\bar{b}$	0.00254±0.00050 /evt
$g \to c\bar{c}$	0.0299±0.0039 /evt
B^0 mass	5.2794± 0.0005 GeV/c^2
b, c hadron lifetimes, R_b, R_c	[15]

Table 1: Uncertainty source and range of variation.

Acknowledgements

We thank the personnel of the SLAC accelerator department and the technical staffs of our collaborating institutions for their outstanding efforts on our behalf.

*Work supported by Department of Energy contracts:
DE-FG02-91ER40676 (BU), DE-FG03-91ER40618 (UCSB), DE-FG03-92ER40689 (UCSC),
DE-FG03-93ER40788 (CSU), DE-FG02-91ER40672 (Colorado), DE-FG02-91ER40677 (Illinois),
DE-AC03-76SF00098 (LBL), DE-FG02-92ER40715 (Massachusetts), DE-FC02-94ER40818 (MIT),
DE-FG03-96ER40969 (Oregon), DE-AC03-76SF00515 (SLAC), DE-FG05-91ER40627 (Tennessee),
DE-FG02-95ER40896 (Wisconsin), DE-FG02-92ER40704 (Yale);
National Science Foundation grants:
PHY-91-13428 (UCSC), PHY-89-21320 (Columbia), PHY-92-04239 (Cincinnati),
PHY-95-10439 (Rutgers), PHY-88-19316 (Vanderbilt), PHY-92-03212 (Washington);
The UK Particle Physics and Astronomy Research Council (Brunel, Oxford and RAL);
The Istituto Nazionale di Fisica Nucleare of Italy
(Bologna, Ferrara, Frascati, Pisa, Padova, Perugia);
The Japan-US Cooperative Research Project on High Energy Physics (Nagoya, Tohoku);
The Korea Research Foundation (Soongsil, 1997).

References

[1] SLD Collab., K. Abe *et al.*, Phys. Rev. Lett. **84** (2000) 4300.
SLD Collab., K. Abe *et al.*, Phys. Rev. **D65**:092006 (2002).

[2] P.N. Burrows, P. Hoyer, V. Del Duca, Z. Phys. **C53** (1992) 149.

[3] SLD Design Report, SLAC Report 273 (1984).

[4] SLD Collaboration, K. Abe *et al.*, Phys. Rev. **D51** (1995) 962.

[5] M.D. Hildreth *et al.*, IEEE Trans. Nucl. Sci. **42** (1994) 451.

[6] C.J.S. Damerell et. al., Nucl. Instr. Meth. **A400** (1997) 287.

[7] S. Brandt *et al.*, Phys. Lett. **12** (1964) 57.
E. Farhi, Phys. Rev. Lett. **39** (1977) 1587.

[8] D. Axen *et al.*, Nucl. Inst. Meth. **A328** (1993) 472.

[9] T. Sjöstrand, Comput. Phys. Commun. **82** (1994) 74.

[10] P. N. Burrows, Z. Phys. **C41** (1988) 375.
OPAL Collab., M.Z. Akrawy *et al.*, Z. Phys. **C47** (1990) 505.

[11] SLD Collab., K. Abe *et al.*, SLAC-PUB-7117; to appear in Phys. Rev. Lett.

[12] R. Brun *et al.*, Report No. CERN-DD/EE/84-1 (1989).

[13] D. J. Jackson, Nucl. Inst. and Meth. **A388**, 247 (1997).

[14] D. Dong, Ph. D. thesis, Massachusetts Institute of Technology, SLAC-Report-550 (1999).

[15] ALEPH, CDF, DELPHI, L3, OPAL, SLD Collabs., CERN-EP/2001-050 (2001).

**List of Authors

Koya Abe,[24] Kenji Abe,[15] T. Abe,[21] I. Adam,[21] H. Akimoto,[21] D. Aston,[21] K.G. Baird,[11] C. Baltay,[30] H.R. Band,[29] T.L. Barklow,[21] J.M. Bauer,[12] G. Bellodi,[17] R. Berger,[21] G. Blaylock,[11] J.R. Bogart,[21] G.R. Bower,[21] J.E. Brau,[16] M. Breidenbach,[21] W.M. Bugg,[23] D. Burke,[21] T.H. Burnett,[28] P.N. Burrows,[17] A. Calcaterra,[8] R. Cassell,[21] A. Chou,[21] H.O. Cohn,[23] J.A. Coller,[4] M.R. Convery,[21] V. Cook,[28] R.F. Cowan,[13] G. Crawford,[21] C.J.S. Damerell,[19] M. Daoudi,[21] N. de Groot,[2] R. de Sangro,[8] D.N. Dong,[13] M. Doser,[21] R. Dubois, I. Erofeeva,[14] V. Eschenburg,[12] E. Etzion,[29] S. Fahey,[5] D. Falciai,[8] J.P. Fernandez,[26] K. Flood,[11] R. Frey,[16] E.L. Hart,[23] K. Hasuko,[24] S.S. Hertzbach,[11] M.E. Huffer,[21] X. Huynh,[21] M. Iwasaki,[16] D.J. Jackson,[19] P. Jacques,[20] J.A. Jaros,[21] Z.Y. Jiang,[21] A.S. Johnson,[21] J.R. Johnson,[29] R. Kajikawa,[15] M. Kalelkar,[20] H.J. Kang,[20] R.R. Kofler,[11] R.S. Kroeger,[12] M. Langston,[16] D.W.G. Leith,[21] V. Lia,[13] C. Lin,[11] G. Mancinelli,[20] S. Manly,[30] G. Mantovani,[18] T.W. Markiewicz,[21] T. Maruyama,[21] A.K. McKemey,[3] R. Messner,[21] K.C. Moffeit,[21] T.B. Moore,[30] M. Morii,[21] D. Muller,[21] V. Murzin,[14] S. Narita,[24] U. Nauenberg,[5] H. Neal,[30] G. Nesom,[17] N. Oishi,[15] D. Onoprienko,[23] L.S. Osborne,[13] R.S. Panvini,[27] C.H. Park,[22] I. Peruzzi,[8] M. Piccolo,[8] L. Piemontese,[7] R.J. Plano,[20] R. Prepost,[29] C.Y. Prescott,[21] B.N. Ratcliff,[21] J. Reidy,[12] P.L. Reinertsen,[26] L.S. Rochester,[21] P.C. Rowson,[21] J.J. Russell,[21] O.H. Saxton,[21] T. Schalk,[26] B.A. Schumm,[26] J. Schwiening,[21] V.V. Serbo,[21] G. Shapiro,[10] N.B. Sinev,[16] J.A. Snyder,[30] H. Staengle,[6] A. Stahl,[21] P. Stamer,[20] H. Steiner,[10] D. Su,[21] F. Suekane,[24] A. Sugiyama,[15] A. Suzuki,[15] M. Swartz,[9] F.E. Taylor,[13] J. Thom,[21] E. Torrence,[13] T. Usher,[21] J. Va'vra,[21] R. Verdier,[13] D.L. Wagner,[5] A.P. Waite,[21] S. Walston,[16] A.W. Weidemann,[23] E.R. Weiss,[28] J.S. Whitaker,[4] S.H. Williams,[21] S. Willocq,[11] R.J. Wilson,[6] W.J. Wisniewski,[21] J.L. Wittlin,[11] M. Woods,[21] T.R. Wright,[29] R.K. Yamamoto,[13] J. Yashima,[24] S.J. Yellin,[25] C.C. Young,[21] H. Yuta.[1]

[1] *Aomori University, Aomori, 030 Japan,*
[2] *University of Bristol, Bristol, United Kingdom,*
[3] *Brunel University, Uxbridge, Middlesex, UB8 3PH United Kingdom,*
[4] *Boston University, Boston, Massachusetts 02215,*
[5] *University of Colorado, Boulder, Colorado 80309,*
[6] *Colorado State University, Ft. Collins, Colorado 80523,*
[7] *INFN Sezione di Ferrara and Universita di Ferrara, I-44100 Ferrara, Italy,*
[8] *INFN Laboratori Nazionali di Frascati, I-00044 Frascati, Italy,*
[9] *Johns Hopkins University, Baltimore, Maryland 21218-2686,*
[10] *Lawrence Berkeley Laboratory, University of California, Berkeley, California 94720,*
[11] *University of Massachusetts, Amherst, Massachusetts 01003,*
[12] *University of Mississippi, University, Mississippi 38677,*
[13] *Massachusetts Institute of Technology, Cambridge, Massachusetts 02139,*
[14] *Institute of Nuclear Physics, Moscow State University, 119899 Moscow, Russia,*
[15] *Nagoya University, Chikusa-ku, Nagoya, 464 Japan,*
[16] *University of Oregon, Eugene, Oregon 97403,*
[17] *Oxford University, Oxford, OX1 3RH, United Kingdom,*
[18] *INFN Sezione di Perugia and Universita di Perugia, I-06100 Perugia, Italy,*

[19] *Rutherford Appleton Laboratory, Chilton, Didcot, Oxon OX11 0QX United Kingdom,*
[20] *Rutgers University, Piscataway, New Jersey 08855,*
[21] *Stanford Linear Accelerator Center, Stanford University, Stanford, California 94309,*
[22] *Soongsil University, Seoul, Korea 156-743,*
[23] *University of Tennessee, Knoxville, Tennessee 37996,*
[24] *Tohoku University, Sendai, 980 Japan,*
[25] *University of California at Santa Barbara, Santa Barbara, California 93106,*
[26] *University of California at Santa Cruz, Santa Cruz, California 95064,*
[27] *Vanderbilt University, Nashville,Tennessee 37235,*
[28] *University of Washington, Seattle, Washington 98105,*
[29] *University of Wisconsin, Madison,Wisconsin 53706,*
[30] *Yale University, New Haven, Connecticut 06511.*

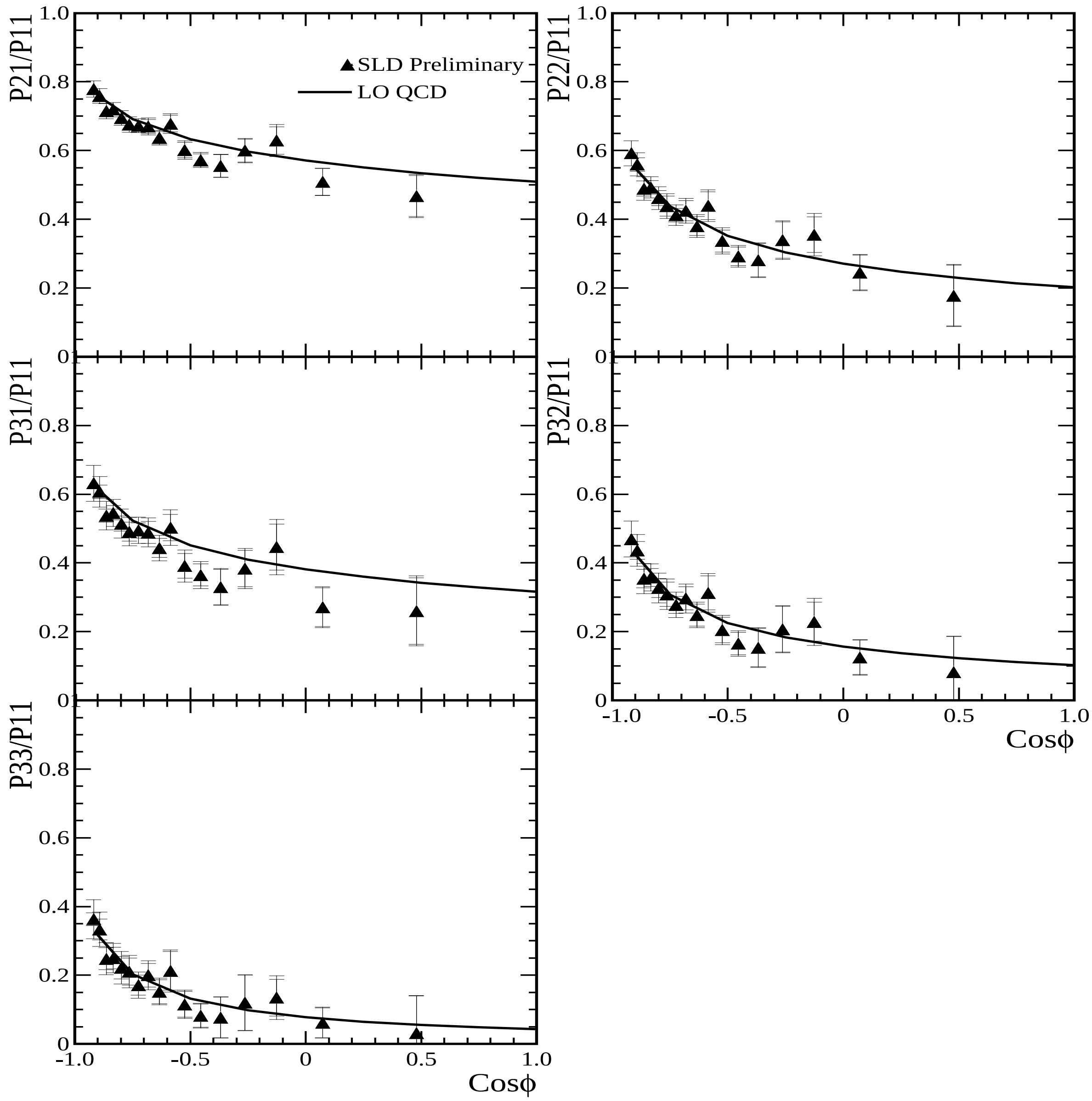

Figure 1: Ratio of moments P_{ij}/P_{11} (see text) vs. $\cos\phi$. Data: points with error bars; the inner error bar represents the statistical error and the outer error bar is the sum in quadrature of the statistical and systematic errors. The lines represent the LO QCD prediction (see text).